

## Effect of tensile strain on the electrical resistivity of silver-coated fly ash cenospheres/silicone-rubber composites

Sheng-Fei Hu · Chong Zhang · Min Zhao ·  
Wen Chen · Shao-Xian Peng

Received: 19 December 2009 / Revised: 15 July 2010 / Accepted: 27 October 2010 /

Published online: 18 November 2010

© Springer-Verlag 2010

**Abstract** Silver-coated fly ash cenospheres were embedded in silicone-rubber to form conductive composites. The electrical resistivity of the composites was examined and compared under different tensile strains. The electrical resistivity was a linear function of tensile strain under quasi-static load at linear viscoelastic area of the composites. Under cyclic strain, the peak of the electrical resistivity decreased and the offset was compared with the peak of strain and stress over time. For the stress relaxation test, the electrical resistivity displayed a change from linear to nonlinear under crescent transient strain. All of the changes were attributed to the breakup and rebuilding of the conductive networks in the composites.

**Keywords** Conductive polymer composites · Tensile strain · Electrical resistivity · Stress relaxation

### Introduction

Due to environmental considerations and rising energy costs, customers have asked for additional requirements on electromagnetic shielding materials [1]. Electrical conductive polymer composites (ECPC) were obtained when particles of good conductors (carbon black, graphite powder, carbon fiber, and microparticles of metals) were implanted into an insulating polymer matrix [2–5], which has become a popular material for electromagnetic shielding over the last decade. The properties

S.-F. Hu (✉) · C. Zhang · M. Zhao · S.-X. Peng  
School of Chemical and Environmental Engineering, Hubei University of Technology,  
Wuhan 430068, People's Republic of China  
e-mail: hghsf@163.com

W. Chen  
School of Materials Science and Engineering, Wuhan University of Technology, Wuhan 430070,  
People's Republic of China

of the materials depend on the atomic and microstructure of the materials. The electrical conductive polymer composites present positive temperature coefficient (PTC) or negative temperature coefficient of resistance (NTC) effect under a temperature field [6], and positive pressure coefficient (PPC) or negative pressure coefficient of resistance (NPC) effect under pressure [7, 8]. New interesting electrical resistivity properties are expected when the composites are stretched under different tensile strains. To enhance electrical conductivity of the materials, it is necessary to increase the ratio of fillers. And the materials will have high density, poor mechanical performance, and high prices [9].

In this article, silver-coated fly ash cenospheres have been selected as electrical conductive particle fillers. The conductive composites have high conductivity, low density and can reduce cost. The studies of the electrical resistance of the conductive composites at different tensile strains centers mainly on obtaining the conductive characteristics for use in electromagnetic shielding applications.

## Experimental

### Materials

Silicone-rubber (ChenGuang Research Institute of Chemical Industry China, 110-2) was used as a matrix. The resistivity is about  $100 \text{ T}\Omega \text{ cm}$ . Silver-coated fly ash cenospheres were obtained by electroplating samples which were produced in the laboratory, with an average diameter of  $34 \mu\text{m}$  and powder density is  $1.793 \text{ g cm}^{-3}$ . Figure 1 shows the SEM micrograph (a) of silver-coated fly ash cenospheres. The surface component of impurities and deposited silver (b) were measured with energy dispersive spectroscopy (EDS).

### Fabrication of test pieces

First, silver-coated fly ash cenospheres and silicone-rubber were mixed in a twin-roll rubber mixing mill at room temperature for 8 min. After a compression molding at  $160^\circ\text{C}$  under 8 MPa for 15 min, the mixture was precured by heating at  $180^\circ\text{C}$

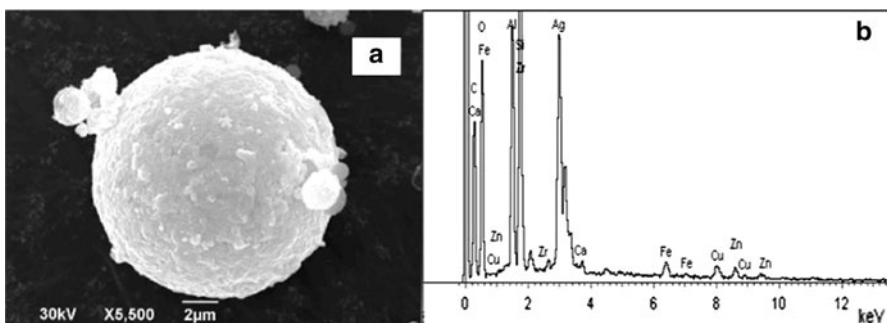


**Fig. 1** SEM micrograph **a** and surface component **b** of silver-coated fly ash cenospheres

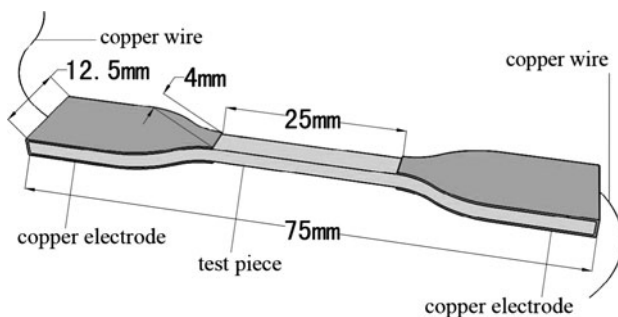


**Fig. 2** Shape and dimensions of test piece

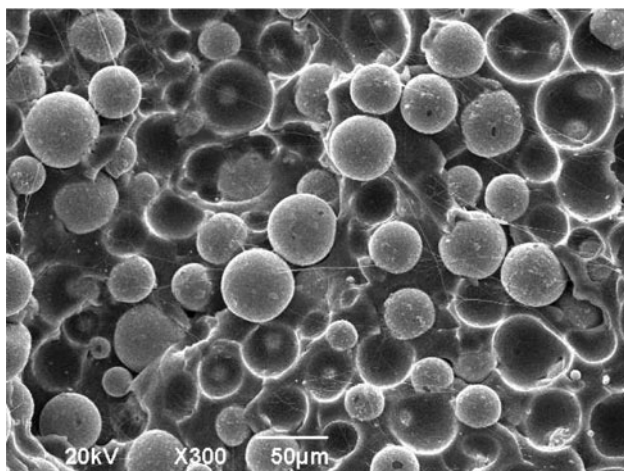


**Fig. 3** Dispersion of silver-coated fly ash cenospheres in silicone-rubber

in an electric blast drying oven for 3 h and cured at 200 °C for 3 h. Finally, the dumbbell-shaped test pieces were cut from the composites by a special knife. Figure 2 shows the shape and dimensions of the test piece with a thickness of 0.86 mm. The volume content of silver-coated fly ash cenospheres in silicone-rubber was 63%. Figure 3 shows the dispersion that silver-coated fly ash cenospheres in silicone-rubber.

### Measurements

Electrical resistance measurements were simultaneously performed along with the mechanical tests. The resistance of the sample was measured with a digital multimeter (UNI-T China, UT804), with the range of 10  $\mu\Omega$ –40 M $\Omega$ . Before the tensile testing, the width and the thickness of the specimens were measured with a micrometer. The electrical resistance of both the copper wires and electrodes was reset before each recording. Tensile tests were performed using a CMT 4000 creep

testing machine (MTS systems) under three types of conditions: (1) under displacement control the samples were stretched to break at the speed of 0.5 mm/min, (2) cyclic tensile strains were calculated to 55, 60, and 65% for up to 20 cycles at the speed of 20 mm/min, (3) the specimens were stretched to tensile strain of 54, 58, and 61% in 1 s, and the displacement was maintained at 1200 s for the stress relaxation. Three specimens of each condition were tested. The microstructures of the samples were observed by SEM (JSM-6390LV, Japan).

## Results and discussion

### Electrical resistance change during sample break

The surface resistance of a sample can be estimated by the well-known relationship given by Ohm's law:

$$R_s = \rho_s \cdot \frac{l}{b} \quad (1)$$

where  $R_s$  is the surface resistance of the sample,  $\rho_s$  is the surface resistivity of the material,  $l$  is the length between contacts, and  $b$  is the width of the middle dumbbell-shaped sample. The electrical resistance change is defined as  $\Delta R/R_0$ :

$$\frac{\Delta R}{R_0} = \frac{\rho_t(1 + \varepsilon) - \rho_0}{\rho_0} \quad (2)$$

where  $\Delta R$  and  $R_0$  are the increased electrical resistance and initial electrical resistance, respectively.  $\varepsilon$  is the tensile strain of the sample,  $\rho_0$  is the initial surface resistivity,  $\rho_t$  is the surface resistivity when strain is the  $\varepsilon$ . Figure 4 shows the relationship between stress, strain, and electrical resistance change obtained during constant tensile speed up to break. The  $\Delta R/R_0$  had a tiny change before 50% strain, and sharply increases from 58 up to  $10^7$  at the strain range of 64–77%. The warp of the electrical resistance change curve due to the conductive networks was destructuralized.

Assuming that the resistivity of each single conductive networks in the sample is equal:

$$\rho_s = \frac{1}{n\mu Q} \quad (3)$$

where  $n$  is the total number of conductive networks,  $Q$  is the charge quantity of each single conductive network and  $\mu$  is the transfer rate of  $Q$  all under the electric intensity of 1. The damage level function of conductive networks  $f(n)$  is used to explain the change of the material electrical resistance in the equation:

$$\frac{\Delta R}{R_0} = f(n)(1 + \varepsilon) - 1. \quad (4)$$

The value of  $f(n)$  tends to be 1 at the composites linear viscoelastic area. Figure 5 shows the relationship between the strain and the resistance change at the

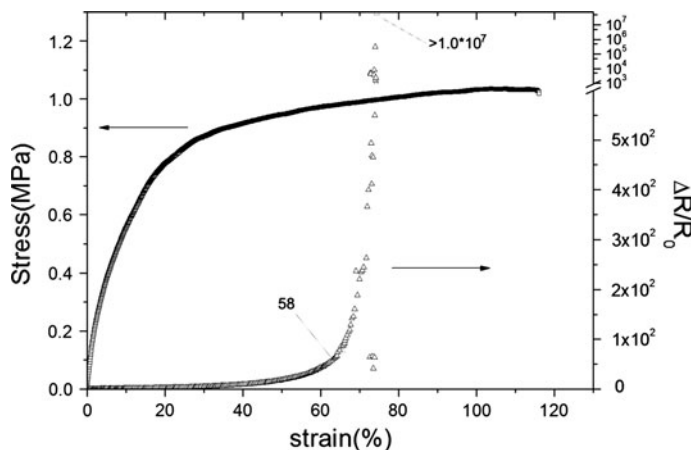


**Fig. 4** Stress and resistance versus strain under constant tensile speed

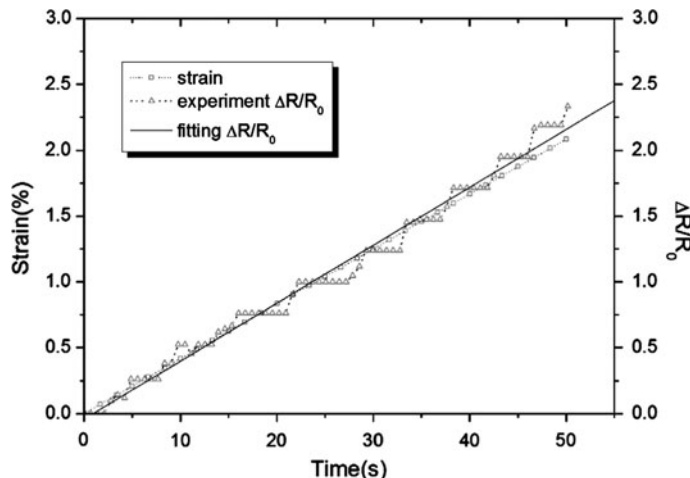


**Fig. 5** The relationship between strain and  $\frac{\Delta R}{R_0}$  at the composites linear viscoelastic area

composites linear viscoelastic area. The curve of the fitting  $\Delta R/R_0$  corresponds to the strain of composites. The ladder phenomenon of resistance change shows that the conductive networks need some time from deformation to breakup. Figure 6 shows the SEM micrographs of surface of the sample before and after tensile testing. The phase separation of matrix and fillers was observed after the tensile test in micrograph (b) compared with the original micrograph (a).

#### Electrical resistance response under cyclic tensile strains

Figure 7 shows the stress and electrical resistance change with tensile loading at increasing strain amplitudes. The strain essentially returned to 30% at the end of

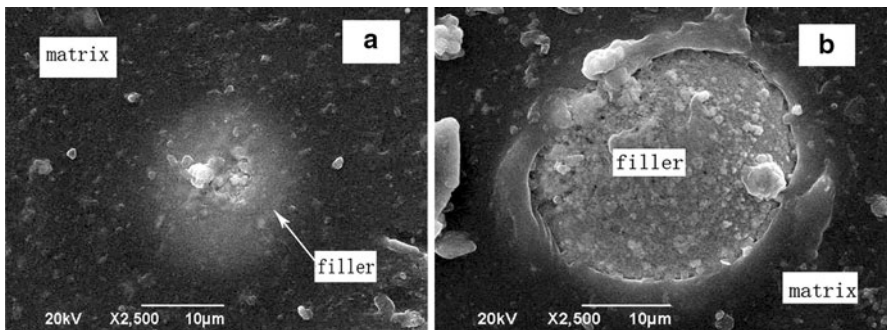


**Fig. 6** SEM micrographs of surface of a composites before **a** and after **b** tensile test

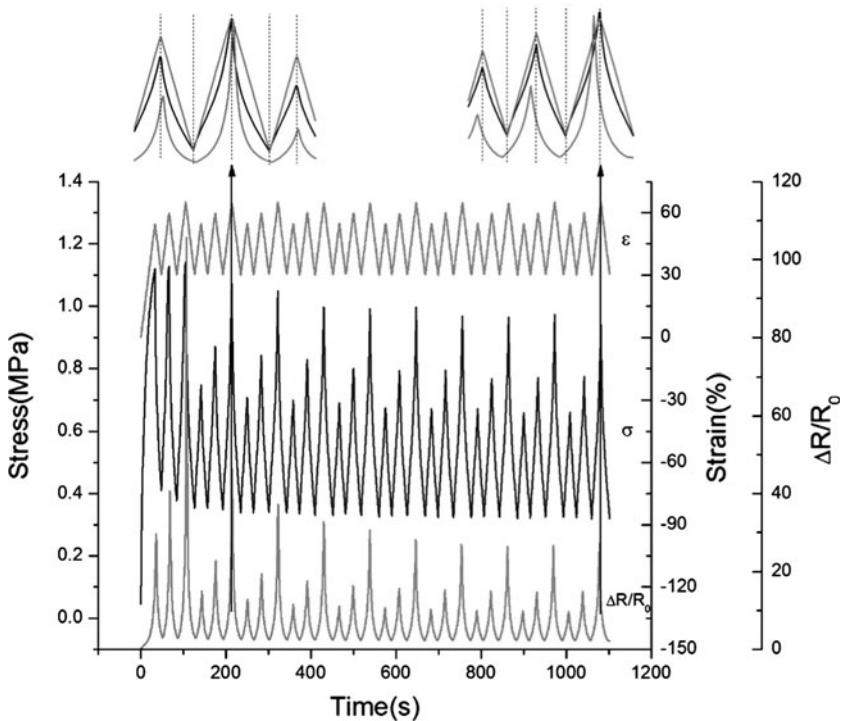


**Fig. 7** Resistance response under cyclic loading

each cycle. The Mullins effect [10] was observed as the peak stress decreased with time. It might be hypothesized that the retraction stresses of an elastomer were independent of silver-coated fly ash cenospheres when the stress at the maximum strain was constant. Under the same strain amplitude, the peak of electrical resistance was very high before the yield stress but decreased over time. As the matrix undergoes cyclic tensile, the decentralized conductive particle cross-linked,

producing more conductive paths. If drawing a vertical line from the peak/valley of electrical resistance curve up to the stress and strain curves, it can be observed that the peak electrical resistance appeared earlier than the peaks stress and strain with increasing time. In the composites system, silver-coated fly ash cenospheres and silicone-rubber were an agglutinate at first, but phase separation will occur under cyclic tensile. As a result, the peaks became offset due to different accelerations between the matrix and the filler movements.

#### Electrical resistance response with stress relaxation behavior

Figure 8 shows the stress relaxation curves and electrical resistance change under different transient tensile strains. The electrical resistance decreased slightly with the material stress relaxation under transient tensile strain of 54% (a) and 58% (b). When the transient tensile strain rose to 61% (c), the electrical resistance curve displayed two peaks before the linear movement decreased. There was a vacancy between 18 and 48 s due to the electrical resistance value that exceeded the measurement range of the digital multimeter. The nonlinear change of the electrical resistance during the constant strain shows that the conductive behaviors of composites were the response to the stress relaxation of silicone-rubber before the critical strain. Under the critical strain, the electrical resistance rose dramatically or significantly since the conductive networks had been broken apart. After a short time, the electrical resistance decreased again with the restoration of the conductive networks as a result of the viscoelastic properties of silicone-rubber. For the second peak, we deduce that the network conductivity responds strongly to the elastic properties of the polymer molecules.

## Conclusions

Silver-coated fly ash cenospheres were embedded in silicone-rubber to form conductive composites. The electrical resistivity of the composites was examined and compared using different tensile strains. Under constant tensile speed, the electrical resistivity was a linear function of the tensile strain within the linear viscoelastic area and then sharply increased at the critical straining of the composites. The step-like changes in the electrical resistance proved that the conductive behavior of the composites depended on the changing network conditions from deformation to destruction. The peak of the electrical resistivity decreased as did the offset with increasing time under cyclic strain due to the rebuilding of prior existing networks containing conductive particles. For the stress relaxation test, the electrical resistivity changed from linear to nonlinear under incremental changes in transient strain. The conductive networks' responsiveness is largely responsible for the silicone-rubber's viscoelastic behavior characteristics as they approach and attain critical strain loading.

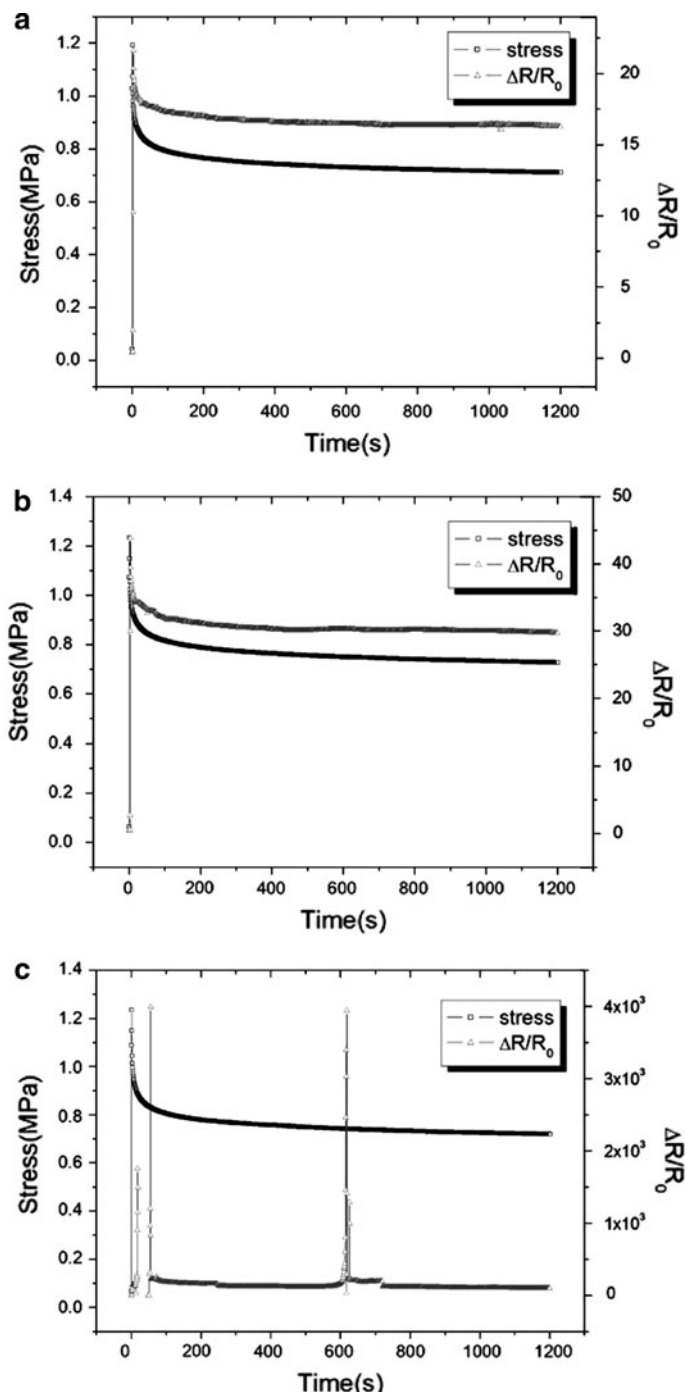


**Fig. 8** Resistance change and stress relaxation at **a** 54%, **b** 58%, and **c** 61% strain

## References

1. Klemperer CV, Maharaj D (2009) Composite electromagnetic interference shielding materials for aerospace applications. *Compos Struct* 91:467
2. Barba AA, Lamberti G, d'Amore M, Acierno D (2006) Carbon black/silicone rubber blends as absorbing materials to reduce Electro Magnetic Interferences (EMI). *Polym Bull* 57:587
3. Saini P, Choudhary V, Sood KN, Dhawan SK (2009) Electromagnetic interference shielding behavior of polyaniline/graphite composites prepared by in situ emulsion pathway. *J Appl Polym Sci* 113:3146
4. Andrzej D (2007) Carbon/polyesterimide thick-film resistive composites—experimental characterization and theoretical analysis of physicochemical, electrical and stability properties. *Microelectron Reliab* 47:354
5. Das A, Stöckelhuber KW, Jurk R, Saphiannikova M, Fritzsche J, Lorenz H, Klüppel M, Heinrich G (2008) Modified and unmodified multiwalled carbon nanotubes in high performance solution-styrene-butadiene and butadiene rubber blends. *Polymer* 49:5276
6. Zhang C, Ma CA, Wang P, Sumita M (2005) Temperature dependence of electrical resistivity for carbon black filled ultra-high molecular weight polyethylene composites prepared by hot compaction. *Carbon* 43:2544
7. Vidhate S, Chung J, Vaidyanathan V, D'Souza N (2009) Time dependent piezoresistive behavior of polyvinylidene fluoride/carbon nanotube conductive composite. *Mater Lett* 63:1771
8. Jeong DY, Ryu J, Lim YS, Dong S, Park DS (2009) Piezoresistive TiB<sub>2</sub>/silicone rubber composites for circuit breakers. *Sens Actuators A Phys* 149:246
9. Agoudjil B, Ibos L, Majesté JC, Candau Y, Mamunya YP (2008) Correlation between transport properties of Ethylene Vinyl Acetate/glass, silver-coated glass spheres composites. *Compos Part A* 39:342
10. Johnson MA, Beatty MF (1993) A continuum mechanics approach to some problems in subcritical crack propagation. *Continuum Mech Thermodyn* 5:301